



Effect of microstructure on strain hardening and strength distributions along a Cr–Ni–Mo–V steel welded joint



Ming-Liang Zhu*, Fu-Zhen Xuan

Key Laboratory of Pressure Systems and Safety, Ministry of Education, School of Mechanical and Power Engineering, East China University of Science and Technology, Shanghai 200237, China

ARTICLE INFO

Article history:

Received 21 July 2014

Accepted 29 September 2014

Available online 8 October 2014

Keywords:

Strain hardening exponent

Hardening stage

Strength prediction

Welded joint

ABSTRACT

Micro-tensile tests based on small-scale specimens were carried out to investigate the microstructure dependence of strain hardening behavior along a Ni–Cr–Mo–V steel welded joint. Results indicated the weld metal (WM) had higher tensile strength but lower strain hardening exponent than base metal (BM), whereas a gradient distribution of strain hardening exponents was observed within the heat-affected zone (HAZ). Bainitic microstructures showed weaker strain hardening capacity than lathy martensites. A Kocks–Mecking type plot of strain hardening rate versus true stress presented at least two hardening stages (stages III and IV) with varied duration along the whole welds. Larger grain size and more lathy martensites were beneficial to prolong the hardening period. A new strength prediction model was developed by considering the size effect on tensile strength. The predicted strength distributions along the welds were in good agreement with experimental data.

© 2014 Elsevier Ltd. All rights reserved.

1. Introduction

According to the ASTM: E646, the tensile strain hardening exponent n is determined by using the Hollomon relation ($\sigma = K\epsilon_p^n$) to describe the plastic flow behavior of metals and alloys in tensile deformation [1]. The exponent n signifies the work hardening potential during plastic deformation while the strength hardening coefficient K indicates the level of strength and formability of the material. Apart from the Hollomon equation, some other stress-strain relationships are used to estimate the plastic deformation behavior [2,3]. Generally, up to four stages of strain hardening has been found when strain hardening rate $d\sigma/d\epsilon$ is plotted with the true stress σ , as documented by Kocks and Mecking [4]. In the past several decades, the strain hardening exponent of various materials has been widely investigated. It is now found that the strain hardening of materials are strongly dependent on the microstructures [5,6], grain size [7,8], temperature [9], and strain rate [10,11].

One of the most important factors is the influence of microstructure on strain hardening behavior. Zhang et al. [12] concluded that the strain hardening of metals was controlled by the mean free path of dislocation motion. When the Ti–6Al–4V alloy was subjected to isothermal compression, the strain hardening exponent was found

to be strongly affected by the strain rate due to the variation of grain size of primary α phase [13]. Research findings still differs in how many stages of the work hardening exist in dual phase steels, though it has been related to different activated deformation mechanisms at strain range corresponding to each stage [14–16]. Movahed et al. [17] found the work hardening exponent enhanced with increasing volume fractions of martensite in a ferrite–martensite dual phase steel, and the volume fraction of martensite was critical to the work hardening stages. The strain hardening investigations on the extruded and equal-channel angularly pressed Mg–Li–Zn alloys concluded that the stacking fault energy played an important role in the disappearance of the stage II hardening [18]. The microstructure is fundamental to understand various hardening behavior among complicated structures, such as welded joints.

The hardening behavior in welded joints has attracted great interests during the past several years. Afrin et al. [19] and Chowdhury et al. [20] reported that the n value in the friction stir welded AZ31B magnesium alloy is nearly twice that of the base metal due to larger grain size after welding. A further study on the SiCp/AA2009 composite joints showed that the hardening potential of the welds increased to about three times that of the base metal [21]. Also of the friction stir welded joints, Cho et al. [22] and Khodaverdizadeh et al. [23] took the strain hardening exponent as a measure to assess the effectiveness of the welding parameters. Motohashi and Hagiwara [24] discussed the influences of material strength matching and strain hardening capacity on the allowable

* Corresponding author. Tel.: +86 21 64251499; fax: +86 21 64253513.

E-mail address: mlzhu@ecust.edu.cn (M.-L. Zhu).

strain and fracture behavior of a X80 line pipe welded joint. Nielson et al. [25] investigated the plastic flow localization in the 6005A aluminum alloy welds and was finally related to the damage development by numerical modelling. The reported results are helpful to understand the plastic flow and fracture behavior of welded joints. However, there is still lack of the distribution of strain hardening behavior along welds, especially in the heat-affected zone (HAZ) where working hardening is difficult to obtain and often neglected. This will involve evaluation of the microstructure influence. Our previous study [26] correlated the weld joint strength well with hardness and microstructures but the strain hardening exponent was determined based on an unverified assumption. Fortunately, the micro-tensile test technique [27] using small size specimens will hopefully give a clear profile of hardening behavior along welded joints.

In the present work, micro-tensile tests will be conducted to investigate the distribution of strain hardening exponents along a Cr–Ni–Mo–V steel welded joint by highlighting the microstructure influences. The hardening exponent results are finally related to the strength distribution of the welds by a revised strength prediction model.

2. Material and experiments

2.1. Material

The material investigated was cut from a 25Cr2Ni2MoV steel welded joint, which was welded by the submerged arc welding (SAW) technique by using a weld metal (WM) whose chemical composition (wt.%) mainly includes Cr 0.69, Mo 0.71, Ni 2.62, C 0.20, Mn 1.63, Si 0.35 and Fe as the balance. The base metal (BM), which has undergone quenching (860 °C) and tempering (630 °C) treatments, has the yield strength (YS) and ultimate tensile strength (UTS) of 768 and 864 MPa, respectively. The chemical composition of the BM in wt.% mainly includes C (0.18–0.27), Si (≤ 0.12), Mn (0.12–0.28), P (≤ 0.015), S (≤ 0.015), Ni (2.05–2.35), Cr (2.15–2.45), Mo (0.63–0.82), V (≤ 0.12), Cu (≤ 0.17) and Fe as the balance. After the SAW process, a post weld heat treatment (PWHT) under furnace cooling was carried out at 580 °C for 10 h to reduce welding residual

stress. The room temperature tensile strength of the welded joint after the PWHT is reduced to 726 and 778 MPa for the YS and UTS, respectively. All failures locate at the BM, indicating the BM is the weakest along the welds. Finally, relatively smaller plate with a size of 300 mm \times 200 mm \times 20 mm was machined from the larger welded rotors for microstructure observation, and tensile and micro-hardness testing.

2.2. Microstructure observation

Surfaces of specimens for optical microscope observations were mechanically polished and then chemically etched in a solution of 4% HNO₃ + ethanol. As indicated in Fig. 1, the width of the WM is about 22 mm, and the width of the HAZ is approximately 3 mm. According to our previous studies [26,27], the HAZ can be further divided into three micro-zones, i.e., fully quenched-tempered zone (FQTZ), partially quenched-tempered zone (PQTZ) and tempered zone (TZ).

2.3. Micro-hardness test

One micro-hardness test specimen was cut from the weld plate with the size of 30 mm \times 10 mm \times 3.6 mm. It was mechanically polished, and then chemically etched in a solution of 4% HNO₃ + ethanol. Micro-Vickers hardness measurements were conducted along the specimen centerline on a hardness tester (HXD-1000TM) at room temperature by holding a test load of 4.9 N for 15 s. Micro-hardness values were directly obtained from the test equipment. The measurement intervals in the HAZ, BM and WM were fixed at 0.2, 0.5 and 1 mm, respectively.

2.4. Micro-tensile test

Tensile tests were performed using micro-specimens which were machined from the WM, BM and sub-zones of the HAZ. The shape and dimensions of the micro-tensile specimens are shown in Fig. 1. The thickness of the micro-tensile test specimen is 0.5 mm. As a result, three or four specimens could be prepared within the HAZ. The tests were carried out on a micro-tensile test

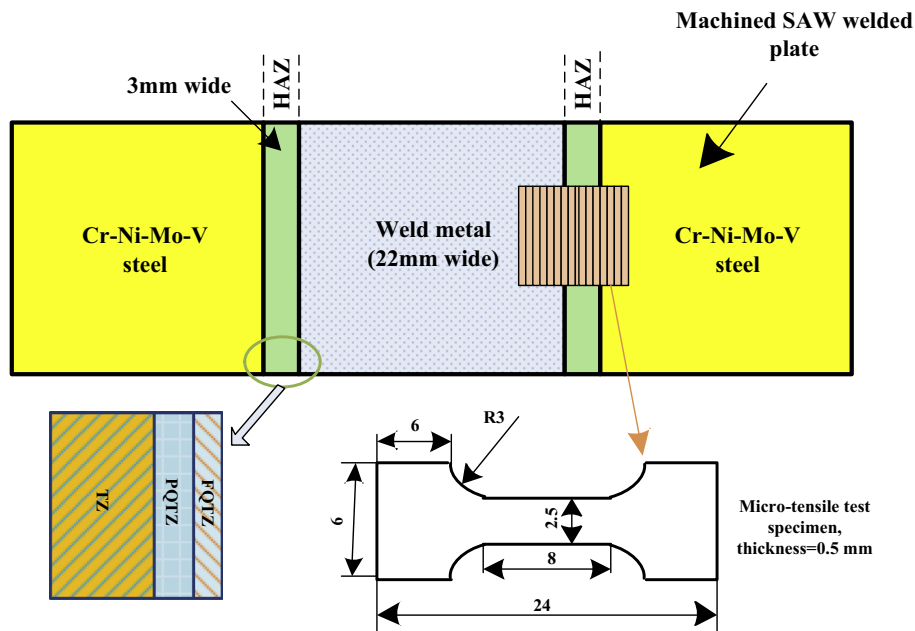


Fig. 1. Schematic of the welded joint and micro-tensile test specimens (dimensions in mm).

Download English Version:

<https://daneshyari.com/en/article/828858>

Download Persian Version:

<https://daneshyari.com/article/828858>

[Daneshyari.com](https://daneshyari.com)